Synthesis, characterization, and antibacterial activity of zinc oxide nanoparticles prepared through pulsed laser ablation

Khalid M. Ali[1], Falah D. Sulaiman[2], and Othman A. Fahad[1]*

ABSTRACT

Although zinc oxide (ZnO) nanoparticles (NPs) are recognized for their antimicrobial properties, little attention has been given to their laser ablation synthesis and antibacterial performance. ZnO NPs were prepared from ZnO metal in distilled water using 300 pulses of a Q-switched laser at variable energy levels (200–500 mJ). The effects of preparation conditions on the structural properties of ZnO NPs were analyzed. X-ray diffraction was used to evaluate the crystallographic structure and crystallite size of the samples, confirming a hexagonal structure consistent with zinc. The band gap of ZnO was found to decrease with increasing laser energy during pulsed laser ablation in liquid due to the increased nanoparticle size and the presence of crystal defects. Scanning electron microscopy images revealed s homogeneous morphology of the ZnO NPs, with diameters ranging from 19.6 to 36.58 nm. Atomic force microscopy analysis demonstrated that increasing laser energy leads to a larger grain size and a corresponding increase in surface roughness. Antibacterial activity of the prepared ZnO NPs was observed against *Staphylococcus aureus* (Gram-positive) and *Escherichia coli* (Gram-negative), confirmed through the agar well-diffusion assay. ZnO NPs prepared at 200 and 300 mJ laser energies exhibited significant inhibitory effects on the growth of all tested bacterial pathogens. This antibacterial activity is attributed to the NPs' large surface area and enhanced surface energy due to their nanoscale size. Findings demonstrate the strong antibacterial potential of laser-synthesized ZnO NPs at low energies, offering a novel perspective on nanomaterial interactions with bacterial pathogens.

Keywords:
ZnO nanoparticles; Antibacterial; *Escherichia coli*; *Staphylococcus aureus*

***Corresponding author:**
Othman A. Fahad,
Othmanabad2@gmail.com

How to cite this article:
Ali KM, Sulaiman FD, Fahad OA. Synthesis, characterization, and antibacterial activity of zinc oxide nanoparticles prepared through pulsed laser ablation. *Biomater Transl.* 2025

doi: 10.12336/bmt.25.00077

1. Introduction

One of the major challenges in modern medicine is deciding whether to use antibiotics or simple therapeutic alternatives for bacterial infections. However, due to the increasing emergence of antibiotic-resistant bacteria, significant efforts have been made to synthesize biologically compatible nanomaterials that can potentially replace antibiotics in antibacterial applications.[1,2] The search for new and practical strategies to combat bacterial diseases has become critical in light of this growing global health threat. Nanomaterials have shown the ability to interact with bacterial cell membranes and interfere with the fundamental cellular processes, largely due to their extremely small size and relatively large surface area.[3] The synthesis and development of materials at the nanoscale, typically with diameters ranging from 1 nm to 100 nm, have enabled tremendous advances in nanotechnology. The chemical and physical properties of nanoparticles (NPs) distinguish them from their bulk counterparts, allowing for exciting applications in various fields.[4-6] These properties, including a high surface-to-volume ratio, quantum effects, and increased biological reactivity, make NPs especially suitable for environmental and medical applications.[7]

Due to their small size and ability to penetrate cell membranes, NPs can directly affect bacteria by disrupting their cell walls, producing reactive oxygen species (ROS), or interfering with vital

intracellular processes.[8] Zinc oxide (ZnO) NPs are among the most promising nanomaterials for antibacterial applications. They have a strong ability to penetrate bacterial cell walls and can damage proteins and DNA by generating ROS, which inhibit or kill the bacteria.[9] Zinc is classified as an n-type semiconductor with a direct band gap of 3.27–3.50 eV. The distinctive properties of ZnO NPs, stemming from their unique crystalline structure and nanoscale dimensions, have made them the subject of extensive research across various scientific domains.[10] NPs have proven effective against both Gram-positive and Gram-negative bacteria, making them suitable for alternative antibiotics, medical applications, and water purification technologies.[11,12] Among the methods for NP synthesis, pulsed laser ablation (PLA) stands out as one of the most efficient and clean techniques. It enables the production of highly pure NPs without the use of chemical additives or impurities, thereby enhancing their biological compatibility and making them ideal for antimicrobial applications.[13,14] In PLA, a high-energy pulsed laser is directed at a target material submerged in a liquid medium, causing vaporization and subsequent condensation into NPs.[15] Evaluating the antibacterial properties of NPs synthesized through PLA against common pathogenic bacterial strains, including *Staphylococcus aureus* (Gram-positive) and *Escherichia coli* (Gram-negative), has become an important research topic.

This study is novel in its elucidation of the relationship among shape, size, and efficacy of antibacterial NPs against *E. coli* and *S. aureus*, depending entirely on variable laser energy levels and antibacterial activity estimate. It represents a significant step toward developing effective nanotechnology-based alternatives for addressing contemporary microbial challenges. The study contributes to the optimization of methods for producing high-quality NPs. The optical, morphological, and structural properties of biosynthesized ZnO NPs, particularly how as well as their effects on bacterial growth, were examined in detail. Advanced characterization techniques, including the effects, were investigated to achieve a deep understanding of the fundamental mechanisms regulating bacterial growth. Atomic force microscopy, X-ray diffraction, ultraviolet (UV)-visible (Vis) spectroscopy, and scanning electron microscopy (SEM) were used for detailed characterization employed to achieve a comprehensive understanding of the mechanisms underlying antibacterial activity.

2. Experimental procedure

ZnO NPs were synthesized using PLA. For ablation, a ZnO target (3 mm in thickness and 10 mm in diameter, purity of roughly 99.8%) in deionized water was obtained from Sigma Aldrich, Germany. NPs were created using a Nd-doped YAG solid-state laser system with of 1064 nm wavelength, delivering 10 ns pulses at a repetition rate of 4 Hz. Laser energies of 200, 300, 400, and 500 mJ were applied. The target-to-laser distance was maintained at 3 cm, as illustrated in **Figure 1**. During ablation, the solution was continuously stirred to ensure uniform NP formation.

2.1. Assessment of antibacterial activity

S. aureus and *E. coli* specimens were obtained from the Department of Microbiology at Mustansiriyah University. Antibacterial activity was assessed using the agar well diffusion method for ZnO NPs synthesized at laser energies of 200 and 500 mJ. Bacterial suspensions were adjusted to match the turbidity of a 0.5 McFarland standard. Each strain was sub-cultured in nutrient broth, and 0.5 mL of ZnO NPs at various concentrations (0.27, 0.30, 0.5, and 0.1 μg/mL) was added. Antibacterial efficacy was evaluated by measuring the zone of inhibition and determining the minimum inhibitory concentration for each sample against both bacterial strains.

3. Results and discussion

3.1. X-ray diffraction analysis

Figure 2 presents an analysis of ZnO NPs synthesized by pulsed laser ablation in liquid (PLAL) at varying laser energy

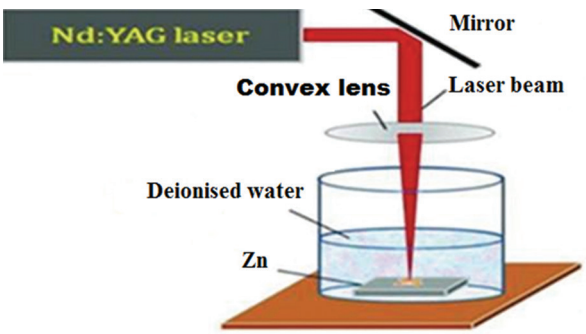

Figure 1. Experimental setup for pulsed laser ablation in a liquid system Abbreviations: Nd: Neodymium; YAG: Yttrium aluminum garnet; Zn: Zinc

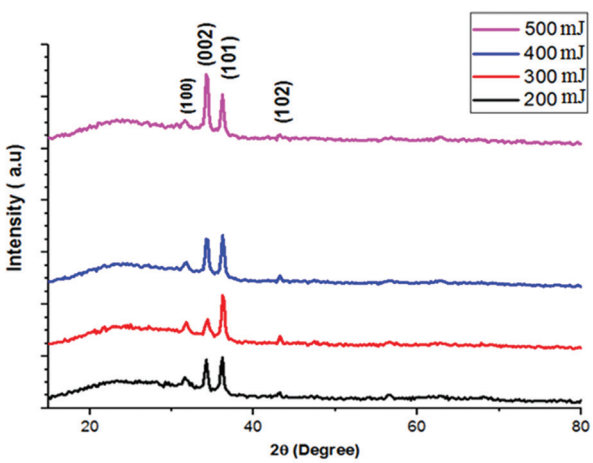

Figure 2. X-ray diffraction of zinc oxide nanoparticles at different laser energy levels

[1]Department of Direction of Education in Al-Anbar, Ministry of Education, Anbar, Iraq; [2]Department of Physics, College of Science, University of Anbar, Ramadi, Anbar, Iraq

levels (200–500 mJ). X-ray diffraction was used to evaluate the crystallographic structure and crystallite size of the samples. Three distinct peaks are observed at 2θ angles corresponding to (100), (002), and (101) planes, which match the hexagonal structure of zinc. This finding indicates that the synthesized NPs possess the same crystal structure as pure ZnO.[16] The crystallite size was determined using the Scherrer equation. Based on the (002) diffraction peak, the crystallite size of the samples prepared at 500 mJ was estimated to be approximately 19.4 nm. As the laser energy increases from 200 mJ to 500 mJ, the intensity of the peaks, especially the (002) peak, also increases. This result indicates that higher laser energy improves the crystallinity of the samples, resulting in a more ordered atomic structure. In addition, the peaks become sharper with increasing laser energy, suggesting an increase in crystallite size and enhanced crystal quality. At lower energies (200 and 300 mJ), the peaks are broader and less intense, corresponding to smaller crystallite sizes (as low as 10.8 nm). The d-spacing remains constant across all energy levels, indicating that the hexagonal crystal phase of ZnO is preserved and unaffected by energy variation. These results show that increasing the laser energy during PLAL improves the crystallinity and quality of ZnO NPs by enlarging the crystallite size and reducing lattice strain, while maintaining structural integrity.

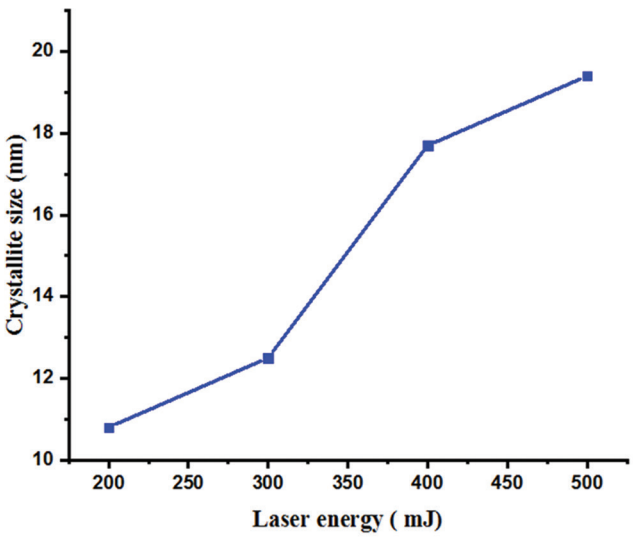

Figure 3. Crystallite size of zinc oxide nanoparticles at different laser energy levels

3.2. Relationship between laser energy and crystallite size

Figure 3 illustrates the relationship between laser energy and the resulting crystallite size of ZnO NPs. A clear trend is observed: crystallite size increases with laser energy, reflecting improved crystallinity and crystal growth under higher ablation energy conditions.

3.3. Optical properties

Figure 4 presents the UV-vis spectra confirming the formation of ZnO NPs synthesized through PLAL at varying energy levels (200–500 mJ). The absorption spectra and corresponding band gap values illustrate the influence of laser energy on the optical properties of the ZnO NPs. The optical band gap of ZnO is observed to decrease with increasing laser energy. This reduction is attributed to an increase in NP size and the presence of crystal defects, which diminish the quantum confinement effect and introduce internal energy levels that lower the optical band gap.[12,17] This phenomenon arises due to the more intense ablation or evaporation of the zinc target at higher laser energies. In addition, defects such as oxygen vacancies or zinc interstitials contribute to the formation of

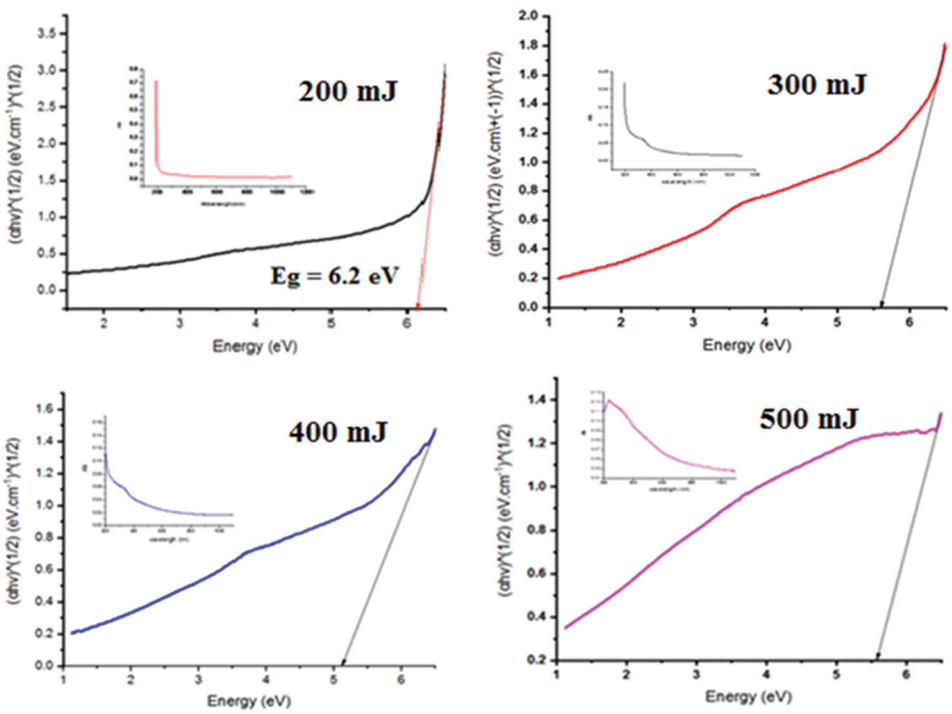

Figure 4. Ultraviolet–visible absorption and band gap of zinc oxide nanoparticles at different laser energy levels

energy states within the band gap, further reducing the band gap energy.[18] A decrease in band gap enhances the absorption of visible light, promotes electron excitation and energy generation, and increases oxygen availability factors that enhance bacterial killing under low light conditions. These effects lead to greater production of electron-vacuum pairs, which react with water and oxygen to form ROS that destroy bacteria. Therefore, a lower band gap improves antibacterial effectiveness even under limited light exposure.[19]

3.4. Relationship between the laser energy and band gap

Figure 5 depicts the inverse relationship between laser energy and the optical band gap of ZnO NPs. As laser energy increases, the energy gap decreases, confirming the role of particle size and defect density in modulating the optical properties of the synthesized NPs.

3.5. SEM analysis

Figure 6 shows SEM images of ZnO NPs prepared at different laser energy levels, highlighting changes in morphology and particle size. The ZnO NPs exhibit a homogeneous distribution, with particle diameters ranging from 19.6 to 36.58 nm. At 200 mJ, the particles appear small and resemble rice grains. At 300 mJ, the particles grow in size and adopt a flower-like morphology, surrounded by smaller, dispersed particles. At 400 mJ, further growth is observed, with particles forming a cauliflower-like structure. At 500 mJ, the surface shows dense particle distribution with overlapping and partial agglomeration. These morphological changes indicate that higher energy laser enhances the rate of ablation from the metal surface and increase particle agglomeration, leading to larger NP sizes. This trend aligns with the findings from both the band gap analysis and X-ray diffraction measurements, confirming a consistent relationship between laser energy, particle size, and crystallinity.

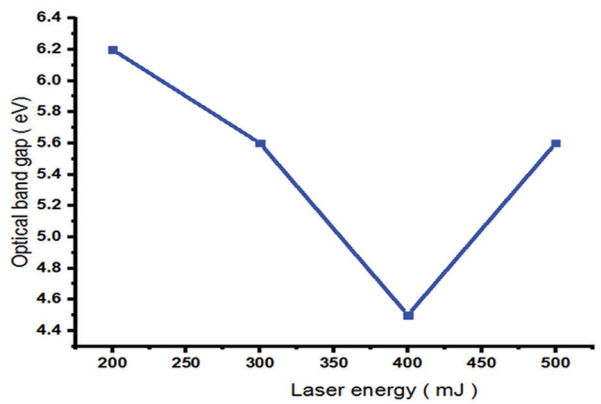

Figure 5. Relationship between optical band gap and laser energy used in nanoparticle synthesis

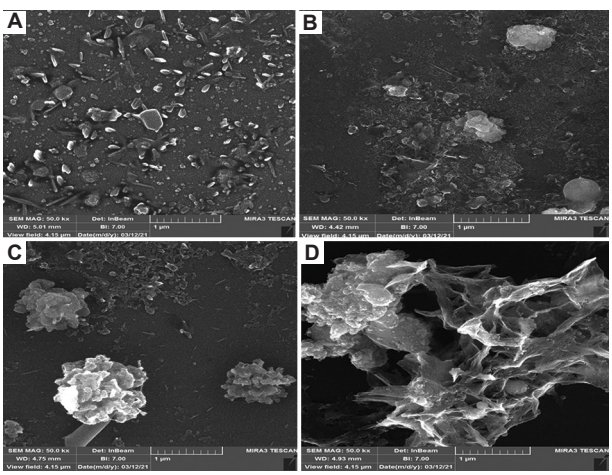

Figure 6. Scanning electron microscopy images of ZnO nanoparticles prepared at variable laser energy levels (A) 200 mJ; (B) 300 mJ; (C) 400 mJ; (D) 500 mJ

3.6. Atomic force microscopy analysis

Figure 7 shows the surface roughness of ZnO NPs. Their bacterial inhibition characteristics were examined using atomic force microscopy. Grain size increases with higher laser energy. The variations in granular size as a function of laser energy are displayed in **Table 1.** As atom mobility on the substrate surface increases due to improved interaction between the ZnO surface and laser energy, average roughness increases with energy level.[20,21] The greater the surface roughness, the higher the likelihood of bacterial adhesion and biofilm formation, which often leads to increased bacterial activity.

At low and medium laser energies, partial dissolution of the surface and particle rearrangement reduce roughness. In contrast, high laser energy may cause rapid evaporation and/or agglomeration of material, increasing particle positioning irregularities and forming bumps that increase roughness.[22]

3.7. Antimicrobial Activity

Figure 8 illustrates the antibacterial activity of ZnO NPs prepared at laser energies of 200, 300, 400, and 500 mJ against *S. aureus* and *E. coli*. The low sensitivity of bacteria to ZnO NPs prepared at high laser energies is attributed to the presence of a murein layer, which hinders NP entry.[23] In addition, increased dislocation and adhesion among NPs at high laser energy seem to impair their penetration into bacterial cell

Table 1. Atomic force microscopy analysis of zinc oxide nanoparticles prepared at variable laser energy levels

Samples	Energies (mJ)	Root mean square (nm)	Average roughness (nm)
ZnO	200	13.20	11.90
ZnO	300	13.80	11.48
ZnO	400	10.40	8.98
ZnO	500	24.10	20.40

Table 2. Antibacterial activity of zinc oxide nanoparticles

Laser energy (mJ)	Inhibition (mm)	
	Staphylococcus aureus	*Escherichia coli*
200	13.5	15
300	17	13
400	0	0
500	0	0

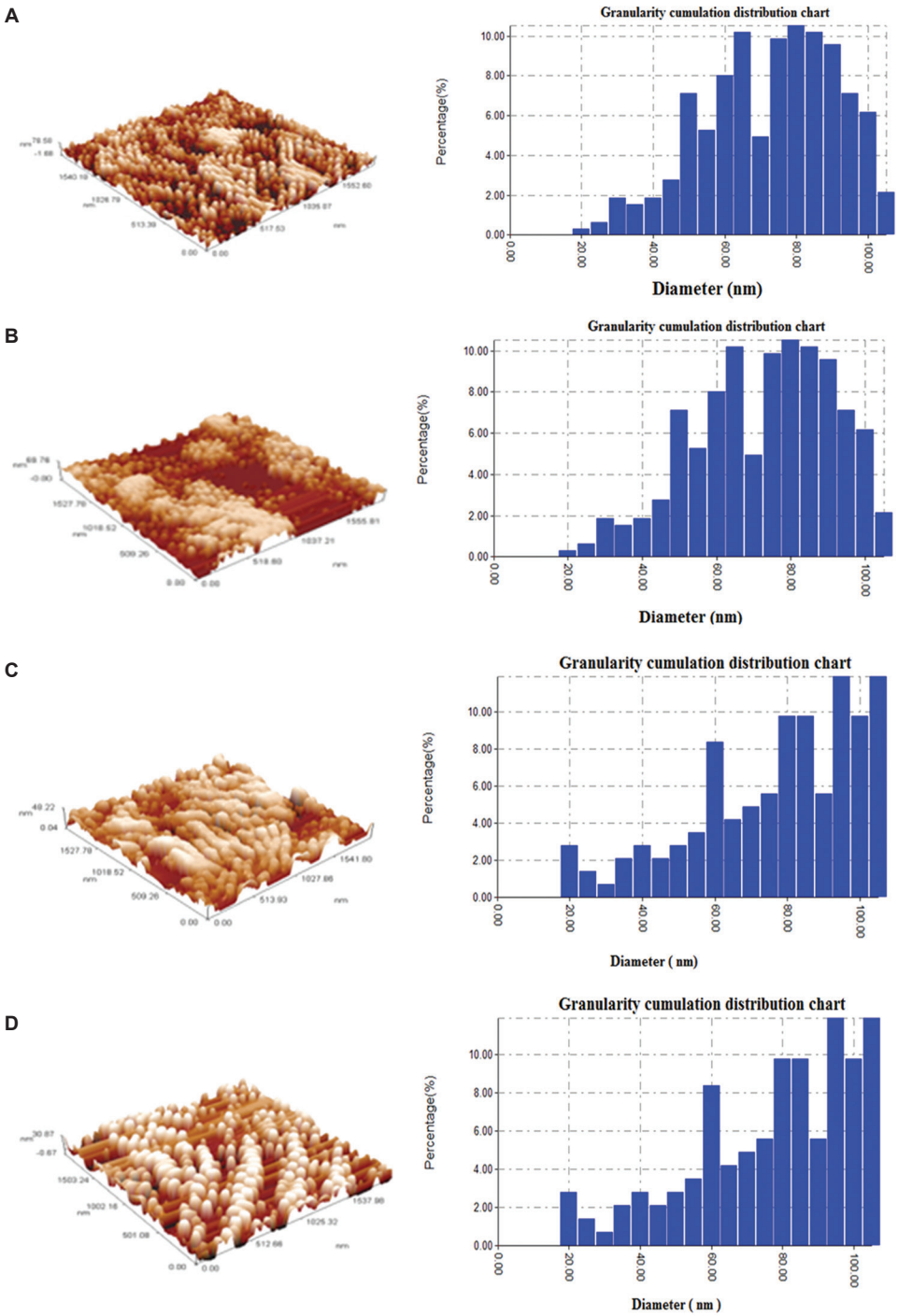

Figure 7. Three-dimensional atomic force microscopy of zinc oxide nanoparticles at variable laser energy levels: (A) 200 mJ; (B) 300 mJ; (C) 400 mJ; (D) 500 mJ. Magnification = 5 × 5μm^2; scale bar = 1 μm.

walls.[24] The antibacterial activity of zinc oxide nanoparticles is shown in **Table 2**. Our results indicate that electrostatic interactions between the ZnO surface and bacterial cell surface significantly contribute to the high antibacterial efficacy of ZnO NPs prepared at lower energy levels (200 and 300 mJ) against both Gram-positive and Gram-negative bacteria. The form, size, and surface-to-mass ratio of the NPs directly affect their antibacterial effectiveness.[25] Because of their large surface-to-volume ratios, smaller NPs offer more effective antibacterial activity. ROS generation at laser energies of 200 and 300 mJ leads to distinct zones of inhibition.[26] The ROS produced by NPs damages bacterial membranes, causes leakage of cytoplasmic contents, DNA damage, and bacterial cell rupture. Cell lysis and collapse are outcomes of the electrostatic interactions between positively charged zinc and the negatively charged bacterial film.[27]

These findings suggest that ROS production induced by ZnO NPs (prepared at 200 and 300 mJ) depends on dose and surface charge, causing oxidative stress, subsequently disrupting bacterial cell membranes, and resulting in cell death.[28] At

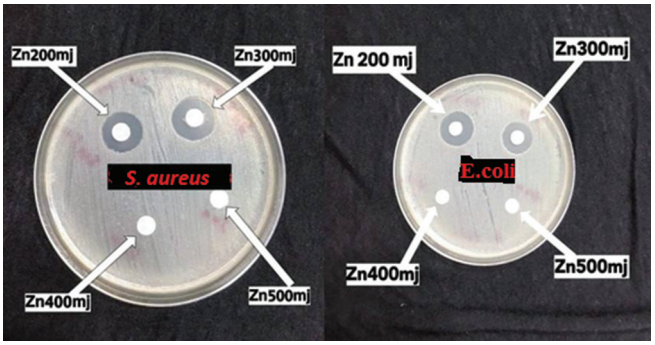

Figure 8. Inhibitory effect of zinc oxide nanoparticles at different laser energy levels

higher zinc concentrations and laser energies, some bacteria exhibit growth resistance.[29] The reduced antibacterial activity of ZnO NPs prepared at high energies (400 and 500 mJ) may result from particle aggregation and changes in NPs shape, which reduce the available surface area for interaction with bacteria.[30] SEM confirms this phenomenon. In addition, the observed resistance in certain bacterial species suggests that antibacterial efficacy cannot be generalized across all species.

The observed inhibition results from direct interaction with bacterial cells, disrupting the permeability of their outer membrane.

4. Limitations

This work has several limitations, including a limited number of experiments and constrained experimental conditions. As a result, the findings may not be fully generalizable. Future research with expanded parameters and additional characterization techniques is necessary to validate and extend these results.

5. Conclusion

High-purity ZnO NPs were successfully synthesized through laser ablation of zinc metal in water. The optical properties of the ZnO NPs were significantly influenced by the laser energy, leading to a reduced energy band gap. The NPs exhibited decreased absorption in the visible and infrared regions, with increased absorption in the UV range. Moreover, the average particle size increased with higher laser energy. ZnO NPs prepared at lower laser energies demonstrated notable antibacterial activity, attributed to their small size and ability to disrupt bacterial cell walls.

Acknowledgement
The authors would like to acknowledge the Plasma Laboratory at the College of Science, University of Anbar, for providing the facilities and technical support necessary to carry out this research.
Financial support
None.
Conflicts of interest statement
The authors declare no conflicts of interest.
Author contributions
Conceptualization: KMA, FDS, and OAF; *Data curation:* OAF; *Formal analysis:* OAF; *Methodology:* OAF; *Visualization:* KMA and FDS; *Writing – original draft:* OAF; *Writing – review & editing:* OAF.
Ethics approval and consent to participate
Not applicable.
Consent for publication
Not applicable.
Availability of data
All data supporting the findings of this study are available upon reasonable request. External data referenced in the manuscript are cited accordingly in the reference list.

References

1. Yousefi M, Dadashpour M, Hejazi M, *et al.* Anti-bacterial activity of graphene oxide as a new weapon nanomaterial to combat multidrug-resistance bacteria. *Mater Sci Eng C Mater Biol Appl.* 2017;74:568-581. doi: 10.1016/j.msec.2016.12.125
2. Lakshmi Prasanna V, Vijayaraghavan R. Insight into the mechanism of antibacterial activity of ZnO: Surface defects mediated reactive oxygen species even in the dark. *Langmuir.* 2015;31(33):9155-9162. doi: 10.1021/acs.langmuir.5b02266
3. Fahad OA. Structural, morphological and antibacterial for cadmium oxide nanoparticles prepared via pulsed laser ablation. *J Optics.* 2024;53:1-8. doi: 10.1007/s12596-024-01072-5
4. Mohammed RS, Al-Marjani MF. Plasma-solution interaction as green pathway to synthesize novel hybrid nanoparticles for medical sterilization (catheter sterilization). *Eur Phys J Plus.* 2025;140(2):156. doi: 10.1140/epjp/s13360-025-06105-6
5. Hasan F, Fahad A, Al-Jenaby Z, Mohammed AS. High performances multi-function of FTO/ZnO/CuO/Al heterojunction device: Gas sensor and solar cell. *J Opt.* 2024;53:1-11. doi: 10.1007/s12596-024-02349-0
6. Fahad A, AlRawi BK, Ramizy A, Salih EY. High-performance ZnO/CdTe/Ge/Si heterojunction photodetector for short/mid-wavelength detection. *Sens Actuators A Phys.* 2025;383:116198. doi: 10.1016/j.sna.2024.116198.
7. Jaffer ZJ, Mazhir SN, Khalaf MK, Hanon MS. Synthesis and surface characterization of PMMA polymer films in pure oxygen, argon, and nitrogen glow discharge plasma. *J Phys Conf Ser.* 2021;1829(1):012010. doi: 10.1088/1742-6596/1829/1/012010
8. Wang ZL. Zinc oxide nanostructures: Growth, properties and applications. *J Phys Condens Matter.* 2004;16(25):R829. doi: 10.1088/0953-8984/16/25/R01
9. Messina GC, Wagener P, Streubel R, *et al.* Pulsed laser ablation of a continuously-fed wire in liquid flow for high-yield production of silver nanoparticles. *Phys Chem Chem Phys.* 2013;15(9):3093-3098. doi: 10.1039/C2CP42626A
10. Mustafa A, AlRashid S. Cohesive energy model for the optical properties in nanostructured materials of zinc sulfide and cadmium selenide. *Chalcog Lett.* 2024;21(5):407-411. doi: 10.15251/CL.2024.215.407
11. AlHada NM, Mohamed Kamari H, Abdullah CA, *et al.* Down-top nanofabrication of binary (CdO)x(ZnO)1-x nanoparticles and their antibacterial activity. *Int J Nanomedicine.* 2017;12:8309-8323. doi: 10.2147/IJN.S150405
12. Kalpana VN, Kataru BAS, Sravani N, Vigneshwari T, Panneerselvam A, Rajeswari VD. Biosynthesis of zinc oxide nanoparticles using culture filtrates of *Aspergillus niger*: Antimicrobial textiles and dye degradation studies. *OpenNano.* 2018;3:48-55. doi: 10.1016/j.onano.2018.06.001
13. Mohammed S, Sudhakaran A, Mostafa MYA, Abbady G. Synthesize of ZnO and CuO nanoparticles with plasma jet at different treatment times and testing its optical parameters with UV-Vis-NIR. *Appl Phys A.* 2024;130(8):533. doi: 10.1007/s00339-024-07651-z
14. Khashan KS, Badr BA, Sulaiman GM, Jabir MS, Hussain SA. Antibacterial

activity of zinc oxide nanostructured materials synthesis by laser ablation method. *J Phys Conf Ser.* 2021;1795(1):012040.
doi: 10.1088/1742-6596/1795/1/012040

15. Hamid NM, Abed HA, Fahad OA. Evaluation of antibacterial effects of silver nanoparticles synthesized via pulsed laser ablation at different laser energies. *Lasers Manuf Mater Process.* 2025;12:488-497.
doi: 10.1007/s42489-025-00123-4
16. Amro NA, Kotra LP, Wadu-Mesthrige K, Bulychev A, Mobashery S, Liu GY. High-resolution atomic force microscopy studies of the *Escherichia coli* outer membrane: Structural basis for permeability. *Langmuir.* 2000;16(6):2789-2796.
doi: 10.1021/la991013x
17. Singh P, Nanda A. Antimicrobial and antifungal potential of zinc oxide nanoparticles in comparison to conventional zinc oxide particles. *J Chem Pharm Res.* 2013;5(11):457-463.
18. Jayaseelan C, Abdul Rahuman A, Vishnu Kirthi A, *et al.* Novel microbial route to synthesize ZnO nanoparticles using *Aeromonas hydrophila* and their activity against pathogenic bacteria and fungi. *Spectrochim Acta A Mol Biomol Spectrosc.* 2012;90:78-84.
doi: 10.1016/j.saa.2012.01.006
19. Haider A, Ijaz M, Imran M, *et al.* Enhanced bactericidal action and dye degradation of spicy roots' extract-incorporated fine-tuned metal oxide nanoparticles. *Appl Nanosci.* 2020;10(4):1095-1104.
doi: 10.1007/s13204-019-01188-x
20. Ahmed B, Hashmi A, Khan MS, Musarrat J. ROS mediated destruction of cell membrane, growth and biofilms of human bacterial pathogens by stable metallic AgNPs functionalized from bell pepper extract and quercetin. *Adv Powder Technol.* 2018;29(7):1601-1616.
doi: 10.1016/j.apt.2018.03.004
21. Mazhir SN, Abdalameer NK, Yaaqoob LA, Hammood JK. Bio-synthesis of (Zn/Se) core-shell nanoparticles by micro plasma-jet technique. *Int J Nanosci.* 2022;21(51):2250041.
doi: 10.1142/S0219581X22500417
22. Haider A, Ijaz M, Imran M, *et al.* Green synthesized phytochemically (*Zingiber officinale* and *Allium sativum*) reduced nickel oxide nanoparticles confirmed bactericidal and catalytic potential. *Nanoscale Res Lett.* 2020;15:50.
doi: 10.1186/s11671-020-3283-5
23. Rajan PI, Vijaya JJ, Jesudoss SK, *et al.* Green-fuel-mediated synthesis of self-assembled NiO nano-sticks for dual applications-photocatalytic activity on rose bengal dye and antimicrobial action on bacterial strains. *Mater Res Express.* 2017;4(8):085030.
doi: 10.1088/2053-1591/aa7e3c
24. Sirelkhatim A, Mahmud S, Seeni A, *et al.* Review on zinc oxide nanoparticles: Antibacterial activity and toxicity mechanism. *Nanomicro Lett.* 2015;7(3):219-242.
doi: 10.1007/s40820-015-0040-x
25. Liedtke J, Vahjen W. *In vitro* antibacterial activity of zinc oxide on a broad range of reference strains of intestinal origin. *Vet Microbiol.* 2012;160(1-2):251-255.
doi: 10.1016/j.vetmic.2012.05.020
26. Ali AH, Shakir ZH, Mezhir A, Mazhir SN. Influence of cold plasma on sesame paste and the nano sesame paste based on co-occurrence matrix. *Baghdad Sci J.* 2022;19(4):855-864.
doi: 10.21123/bsj.2022.19.4.0855
27. Patrinoiu G, Dumitru R, Culita DC, *et al.* Self-assembled zinc oxide hierarchical structures with enhanced antibacterial properties from stacked chain-like zinc oxalate compounds. *J Colloid Interface Sci.* 2019;552:258-270.
doi: 10.1016/j.jcis.2019.05.051
28. Ahmed HO, Yaaqoob LA. Evaluation of antibacterial activity of nickel oxide nanoparticles against *Escherichia coli*. *Iraqi J Agric Sci.* 2025;56(1):502-511.
doi: 10.36103/aws0zt84
29. Eskandari AF, Dorranian D. Effect of laser fluence on the characteristics of ZnO nanoparticles produced by pulsed laser ablation in acetone. *J Nanopart Res.* 2015;17(5):1-9.
doi: 10.1007/s11041-015-1961-6
30. Saeed AA. Structural and optical properties for ZnO nanoparticles for antibacterial application. *Tikrit J Pure Sci.* 2025;30:62-70.
doi: 10.25130/tjps.v30i1.1779

Received: June 28, 2025
Revised: August 29, 2025
Accepted: September 10, 2025
Available online: October 16, 2025